Bioorganic & Medicinal Chemistry 20 (2012) 2829–2836

Contents lists available at SciVerse ScienceDirect

Bioorganic & Medicinal Chemistry

journal homepage: www.elsevier.com/locate/bmc

Disubstituted 1,8-dipyrazolcarbazole derivatives as a new type of *c-myc* G-quadruplex binding ligands

Wei-Jia Chen, Chen-Xi Zhou, Pei-Fen Yao, Xiao-Xiao Wang, Jia-Heng Tan, Ding Li, Tian-Miao Ou, Lian-Quan Gu, Zhi-Shu Huang *

School of Pharmaceutical Sciences, Sun Yat-Sen University, Guangzhou 510006, People's Republic of China

ARTICLE INFO

Article history:
Received 29 January 2012
Revised 13 March 2012
Accepted 14 March 2012
Available online 21 March 2012

Keywords:
G-Quadruplex
c-myc Oncogene
1,8-Dipyrazolcarbazole derivatives
Binding ligand
Selectivity

ABSTRACT

A series of 1,8-dipyrazolcarbazole (DPC) derivatives (**6a**–**6d**, **7a**–**7d**) designed as G-quadruplex ligands have been synthesized and characterized. The FRET-melting and SPR results showed that the DPC derivatives could well recognize G-quadruplex with strong discrimination against the duplex DNA. In addition, the DPC derivatives showed much stronger stabilization activities and binding affinities for *c-myc* G-quadruplex rather than telomeric G-quadruplex. Therefore, their interactions with *c-myc* G-quadruplex were further explored by means of CD spectroscopy, PCR-stop assay, and molecular modeling. In cellular studies, all compounds showed strong cytotoxicity against cancer cells, while weak cytotoxicity towards normal cells. RT-PCR assay showed that compound **7b** could down-regulate *c-myc* gene expression in Ramos cell line, while had no effect on *c-myc* expression in CA46 cell line with NHE III_1 element removed, indicating its effective binding with G-quadruplex on *c-myc* oncogene in vivo.

1. Introduction

G-Quadruplexes are DNA secondary structures formed from planar arrangements of four guanines stabilized by Hoogsteen hydrogen bonding and monovalent cations.[1] G-Quadruplexes have received much attention recently due to their putative existence in telomeres and in the promoter regions of oncogenes such as *c-myc*.[2] Human telomeric DNA, located at the end of chromosomes, consists of tandem repeats of sequence d[$(TTAGGG)_n$], which ends as the single strand.[3] Ligands capable of inducing and stabilizing G-quadruplex formation of these telomeric DNA could inhibit telomerase activity and interference with telomere biology.[4,5] On the other hand, the c-Myc oncoprotein is an important transcription factor that plays a pivotal role in cell proliferation and survival.[6] The nuclear hypersensitivity element III_1 (NHE III_1), upstream of the P1 promoter of *c-myc*, controls 80–90% of the *c-myc* transcription level.[7,8] The NHE III_1, a G (guanine)-rich strand of the DNA containing a 27 base pair sequence, can form intramolecular G-quadruplex structures and functions as a transcriptional repressor element.[9] The transcription of *c-myc* can be inhibited by the stabilization of G-quadruplexes by using specific G-quadruplex binders. Several small molecular ligands have been reported to stabilize G-quadruplex, including cationic porphyrins, quindoline derivatives, and platinum complexes.[10–12] These aromatic moieties π-stack onto the terminal tetraplex of the quadruplex providing extra stabilization.[13,14] Their side chains usually have positive charge, or can become protonated at physiological pH, which is another common feature of providing electrostatic interactions with the negatively charged phosphate residues in the grooves.[15]

Some carbazole alkaloids have been isolated from *Clausena harmandiana* and *Clausena excavate*, which have shown significant cytotoxicity against cancer cell lines.[16,17] Recently, a carbazole derivative, 3,6-bis(1-methyl-4-vinylpyridinium) carbazole diiodide (BMVC), has been found to be a good G-quadruplex stabilizer, which has shown an increase in G-quadruplex melting temperature by 13 °C and has had a potent inhibitory effect on telomerase activity.[18] So we think that the molecular architecture of carbazole offers an attractive template for the design of G-quadruplex binding ligand. Besides, previous studies have shown that expanding the size of aromatic planar surface of molecules might enhance their binding potency and selectivity on G-quadruplex DNA over duplex DNA, because square aromatic surface of G-quartet is much larger than that of the Watson–Crick base pairs.[19,20] We hypothesized that introduction of other aromatic groups to carbazole core could further improve its quadruplex stabilizing property. It should be mentioned that pyrazole has been found as a pharmacophore in some active biological molecules, and pyrazole derivatives have been extensively studied as anticancer,[21,22] anti-inflammatory,[23] and antimicrobial[24,25] molecules. The pyrazole ring represents a good pharmacophore for the synthesis of biologically active compounds with varying activity and good safety profiles. Therefore, we designed a series of 1,8-dipyrazolcarbazole (DPC) derivatives,

* Corresponding author. Tel./fax: +86 20 39943056.
E-mail address: ceshzs@mail.sysu.edu.cn (Z.-S. Huang).

0968-0896/$ - see front matter © 2012 Elsevier Ltd. All rights reserved.
http://dx.doi.org/10.1016/j.bmc.2012.03.031

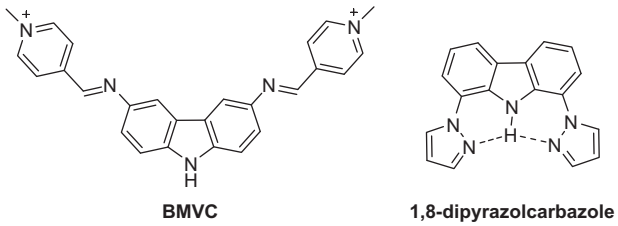

Figure 1. Structures of BMVC and 1,8-dipyrazolcarbazole.

which had two pyrazole groups for enhancing their anticancer activity through their π–π stacking interactions with G-quadruplex. As shown in Figure 1, intramolecular hydrogen bond is formed in these designed molecules, which improves the planarity of the molecular structure through enhanced π-delocalization. Two cationic side chains of the 1,8-dipyrazolcarbazole core could interact with the grooves and loops of the G-quadruplex, which may be necessary to enhance its G-quadruplex binding potency and selectivity, as well as its aqueous solubility. The interactions between the DPC derivatives and *c-myc* G-quadruplex were examined by a series of biophysical and biochemical methods.

2. Results and discussion

2.1. Chemistry

The synthetic pathway for the DPC derivatives was shown in Scheme 1. Nitration of carbazole with cupric nitrate, acetic acid and acetic anhydride gave a mixture of 1-nitro-, 1,6-dinitro-, and 3,6-dinitrocarbazoles from which the desired 3,6-dinitrocarbazole **2** could be isolated by using chromatography.[26] The 1,8-dibromo-3,6-dinitrocarbazole **3** was obtained through the reaction of 3,6-dinitrocarbazole **2** with bromine in sulfuric acid.[27] The 1,8-dibromo-3,6-dinitrocarbazole **3** was then coupled with pyrazole to give 1,8-dipyrazol-3,6-dinitrocarbazole **4**. A large excess of pyrazole had to be used, but it was possible to recycle this material.[28] The reduction of 1,8-dipyrazol-3,6-dinitrocarbazole **4** with tin powder and hydrochloric acid produced intermediate 1,8-dipyrazol-3,6-diaminocarbazole, which was reacted with acyl chloride to give compounds **5a**–**5b**.[26] Finally, the desired products **6a–6d** and **7a–7d** were obtained through aminolysis of the compounds **5a** and **5b** with appropriate secondary amines under reflux.

2.2. Studies for the stabilization and selectivity of the DPC derivatives on G-quadruplex with FRET assays

The effect of the DPC derivatives on the stabilization of G-quadruplex was evaluated by using a FRET-melting assay.[29] The human telomeric G-quadruplex DNA (F21T) and the oncogene promoter G-quadruplex *c-myc* (FPu18T) were used in this assay. The results of the FRET-melting experiments were shown in Table 1, which indicated that these compounds had a wide range of G-quadruplex stabilization activity towards telomeric G-quadruplex and *c-myc* G-quadruplex. The compounds with longer side chains showed better G-quadruplex stabilizing properties except those with morpholine terminal group. The difference of the ΔT_m values could be caused by several reasons, for example, compound **6d** and **7d** had two morpholine rings on the side chains, the oxygen atom on the morpholine ring made compound **6d** and **7d** more polar than the others, the basicity of side chain amines was different.[30,31] Similar results had been obtained for tri-substituted isoalloxazine and triarylpyridine derivatives,[32] and the derivatives with a morpholine ring on the side chain had lower ΔT_m values than those with amino alkyl side chains. On the other hand, it should be mentioned that these compounds showed stronger effect on the thermal stability of *c-myc* G-quadruplex (ΔT_m: 4.4–18.1 °C) than telomeric G-quadruplex (ΔT_m: 1.2–11.9 °C).

FRET-melting experiments were also used to examine the binding selectivity of the compounds. F10T (5′-FAM-dTATAGCTATA-HEG-TATAGCTATA-TAMRA-3′) is a self-complementary hairpin duplex DNA.[33] As shown in Table 1, the derivatives showed weak effect on the thermal-stability of the duplex DNA F10T (ΔT_m <1 °C), suggesting their poor binding with the duplex DNA. To further characterize the selectivity of these ligands for G-quadruplex, competitive FRET experiment was carried out, and a duplex oligomer ds26 (5′-CAATCGGATCGAATTCGATCCG-ATTG-3′) was used in this study.[34] Excess duplex DNA ds26 was mixed with *c-myc* G-quadruplex FPu18T before FRET-melting assay with ligands for ΔT_m values determination. The result of competitive FRET-melting assay was shown in Figure 2, and the ΔT_m values for compounds were not significantly decrease, which indicated that the DPC derivatives could specifically stabilize *c-myc* G-quadruplex without significant effect for duplex DNA.

2.3. Studies for the binding and selectivity of the DPC derivatives on G-quadruplex with Surface Plasmon Resonance

Surface Plasmon Resonance (SPR) experiments were carried out to study the interactions between DPC derivatives and G-quadruplex quantitatively (Fig. S2). [35] As shown in Table 1, compounds **6a–6c**, **7a–7c** exhibited high affinities for *c-myc* G-quadruplex and telomeric G-quadruplexes. No obvious binding was found for compounds **6d** and **7d** even at concentration of 20 μM, which was consistent with very low ΔT_m values obtained from FRET melting experiment. SPR experiments also indicated that compounds with longer side chains showed higher G-quadruplex binding affinities except compounds with morpholine terminal group. In addition, the carbazole derivatives showed much stronger binding affinities for *c-myc* G-quadruplex than telomeric G-quadruplex. For example, compounds **7a** showed more than 20 times binding affinity for *c-myc* G-quadruplex over telomeric G-quadruplex. For the study of their binding affinities for duplex DNA, the incubation of these compounds with duplex DNA immobilized on the chips showed no significant binding interactions. These results were in parallel with FRET-melting data showing the DPC derivatives can be considered as a new class of selective G-quadruplex binding ligands.

From both FRET-melting and SPR results, the DPC derivatives showed much stronger stabilization activities and binding affinities for *c-myc* G-quadruplex rather than telomeric G-quadruplex. Therefore, the interaction of the DPC derivatives *and c-myc* G-quadruplex was further explored by means of CD spectroscopy, PCR-stop assay, and molecular modeling.

2.4. Studies of the binding property of the DPC derivatives on *c-myc* G-quadruplex with Circular Dichroism

To further confirm the above results, and determine the conformational change of G-quadruplex induced by the DPC derivatives, Circular Dichroism (CD) experiment was carried out.[36] CD spectroscopy was used to examine the effect of **7a**, **7b** and **7c** on *c-myc* G-quadruplex in the presence and absence of stabilizing salt. Oligonucleotide Pu18 (5′-AGGGTGGGGAGGGTGGGG-3′) was used as the *c-myc* sequence. As shown in Figure 3A, in the presence of 100 mM K^+, Pu18 showed a positive signal at about 262 nm and a negative signal at 240 nm, which suggested a typical parallel G-quadruplex structure. Upon addition of compounds to Pu18, no significant change was observed, which indicated that the DPC derivatives could still maintain the parallel *c-myc* G-quadruplex structure in the presence of potassium ion.

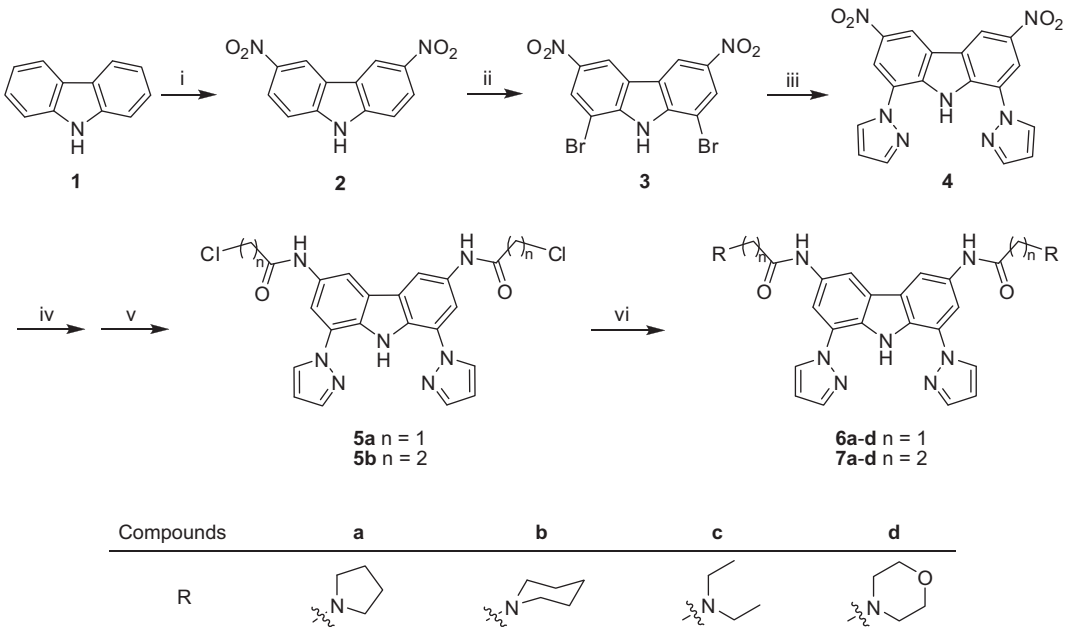

Scheme 1. Synthesis of the DPC derivatives. Reagents and conditions: (i) $Cu(NO_3)_2$, acetic anhydride, acetic acid (90 °C); (ii) Br_2, concentrated H_2SO_4 (90 °C); (iii) pyrazole, Cu_2O, *N*-methyl-2-pyrrolidone, Ar (200 °C); (iv) Sn, concentrated HCl, acetic acid (reflux); (v) chloroacetyl chloride or 3-chloropropionyl chloride (70 °C); (vi) substituted alkylamine, EtOH (reflux).

Table 1
G-Quadruplex stabilization (ΔT_m) potential obtained from FRET-melting and equilibrium binding constants (K_D) measured with SPR

Compounds	FRET (ΔT_m/°C)[a]			SPR (K_D/μM)		
	FPu18T	F21T	F10T	Pu18	HTG21	Duplex
6a	9.3	6.3	0.3	0.694	2.97	—[b]
6b	5.5	4.0	0.1	1.46	8.07	—[b]
6c	7.4	3.6	0.6	2.03	6.86	—[b]
6d	4.4	1.2	0.2	—[b]	—[b]	—[b]
7a	15.1	10.7	0.5	0.131	2.64	—[b]
7b	12.1	9.7	0.3	0.135	1.88	—[b]
7c	18.1	11.9	0.3	0.233	2.59	—[b]
7d	7.3	4.2	0.3	—[b]	—[b]	—[b]

[a] $\Delta T_m = T_m$ (DNA + ligand) − T_m (DNA). The concentrations of FPu18T, F21T, and F10T were 0.2 μM, and the concentrations of compounds 1.0 μM.
[b] No significant binding was found for addition of up to 20 μM ligand, which might indicate no specific interactions between the ligand and the DNA.

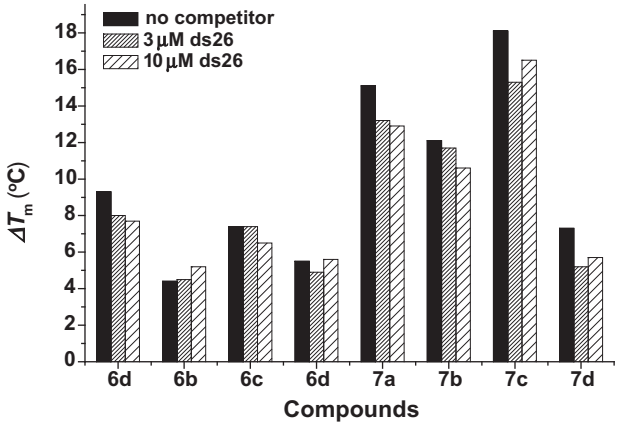

Figure 2. Competitive FRET results for the DPC derivatives (1 μM), without and with 15-fold (3 μM) or 50-fold (10 μM) excess of duplex DNA competitor (ds26). The concentration of FPu18T was 0.2 μM.

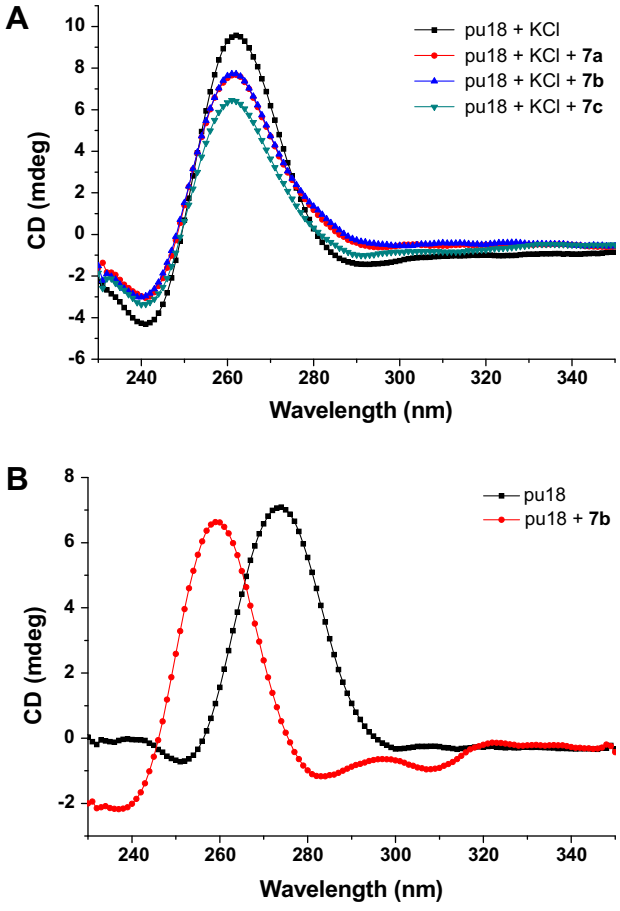

Figure 3. (A) Change of the CD spectra of Pu18 in the presence of KCl. The concentrations of **7a**, **7b** and **7c** were 25 μM. The concentration of the Pu18 remained at 5 μM in 10 mM Tris–HCl buffer, 100 mM KCl, pH 7.2. (B) Change of the CD spectra of Pu18 in the absence of KCl. The concentration of **7b** was 25 μM. The concentration of the Pu18 remained at 5 μM in 10 mM Tris–HCl buffer, pH 7.2.

The CD spectroscopy of Pu18 in the absence of metal ion was also studied. As shown in Figure 3B, The CD spectra of Pu18 without any metal cation exhibited a small negative peak at 250 nm and a large positive peak at 275 nm. After the treatment with **7b** (25 μM), the positive peak shifted to 262 nm while the negative peak shifted to 240 nm. These changes in the CD spectra indicated that **7b** could effectively induce conformational change of G-quadruplex.

2.5. Molecular modeling studies

To further investigate the mode of binding, molecular modeling for the binding of **7a** on the model of the NHE III_1 intramolecular G-quadruplex loop isomer was performed. Nucleotides G2–G5 in the Pu27-mer were not involved in the G-quadruplex structure, so the truncated sequence Pu18-mer (A6-G23 in Pu27-mer) was used for subsequent studies. The previously built Pu-18B G-quadruplex structure was used as the initial model to study the interaction between compounds and human *c-myc* G-quadruplex DNA.[37] Our results showed that **7a** could stack on both external G-quartet planes. Preferable binding site of **7a** was found to be 5′-terminal G-quartet plane, with a calculated binding energy of −8.3 kcal/mol. As shown in Figure 4, the ligand molecule effectively filled much of the space in the plane of the G-quartet between the phosphate groups. The two positively-charged side chains were properly oriented and directed into the DNA groove towards the negatively charged phosphate diester backbone, and formed electrostatic interactions and hydrogen bonds.

2.6. Inhibition of amplification in the promoter region of *c-myc* by the DPC derivatives

To get quantitative estimates of G-quadruplex stabilization by the DPC derivatives, PCR stop assay was performed.[37,39] Pu27 (5′-TGGGGAGGGTGGGGAGGGTGGGGAAGG-3′) was chosen as the testing oligonucleotide. The formation of the G-quadruplex can block its hybridization with a complementary strand and leads to the double-stranded DNA PCR product being undetectable. The results were shown in Figure 5 and Table 2. Compounds **6a**, **7a–c** showed high inhibitory effect on the hybridization of Pu27, and their IC_{50} values ranged from 3.6 to 6.3 μM. Other compounds showed weak inhibitory effect on the hybridization of Pu27 (IC_{50} >20 μM). These results were correlated with the ΔT_m values and binding affinities obtained from SPR in Table 1, indicating that the stability and binding interactions on *c-myc* G-quadruplex induced by these compounds were important for inhibiting PCR amplification. The pyrrolidine group of **6a** or **7a** was optimal for their interactions with G-quadruplex, while the morpholine group of **6d** or **7d** was unfavorable for the binding interaction.

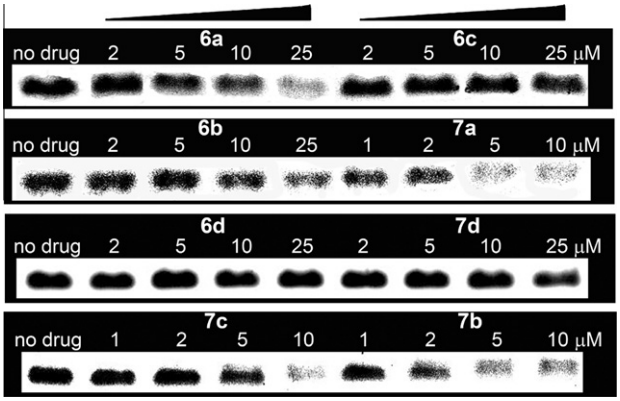

Figure 5. Effects of the DPC derivatives **6a–d**, **7a–d**, on the hybridization of the Pu27 in the PCR-stop assay.

Table 2
The IC_{50} values of the DPC derivatives in PCR-stop assay

Compounds	6a	6b	6c	6d	7a	7b	7c	7d
IC_{50} (μM)	5.2	>20	>20	>20	3.6	4.9	6.3	>20

2.7. MTT assay

By using an MTT assay, the cytotoxicity of compounds against HL60, HepG2, and NCI-H460 cancer cell lines was determined, while their toxicity to normal cells was evaluated by using the normal cell line ECV-304 (Table 3). All compounds displayed strong cytotoxicity against cancer cells, but showed a weak cytotoxicity against normal epithelial cell ECV-304, indicating that all the derivatives had relatively good selectivity on tumor cells, although some of them had little effect on *c-myc* G-quadruplex binding and stabilization, which may be due to other factors.

2.8. Inhibition of *c-myc* expression in cancer cell line

A reverse transcriptase-polymerase chain reaction (RT-PCR) was performed to determine the impact of complexes on the mRNA level of *c-myc* oncogene.[37] Two Burkitt's lymphoma cell

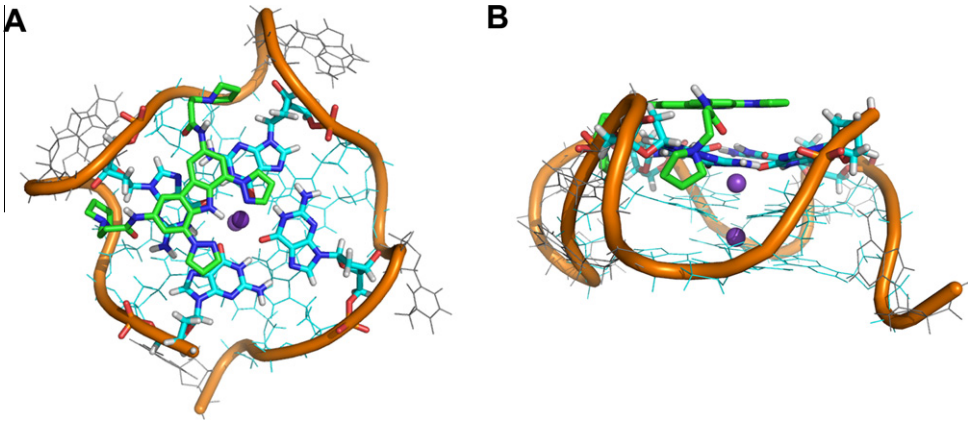

Figure 4. Top view (A) and side view (B) of compound **7a** forming π–π stacking interactions with the 5′ G-quartet. The ligand side chains are directing in the grooves. Pictures were generated by PYMOL.[38]

Table 3
IC_{50} values (μM) of the DPC derivatives against tumor cells

Compounds	HL60	NCI-H460	HepG2	ECV-304
6a	1.9	2.7	2.7	22.2
6b	2.4	3.3	5.6	27.3
6c	2.0	2.5	3.0	22.8
6d	3.9	3.9	6.1	29.3
7a	2.2	3.5	4.2	25.2
7b	1.2	2.7	5.1	25.0
7c	1.9	2.6	2.7	23.3
7d	1.7	2.8	6.9	26.2

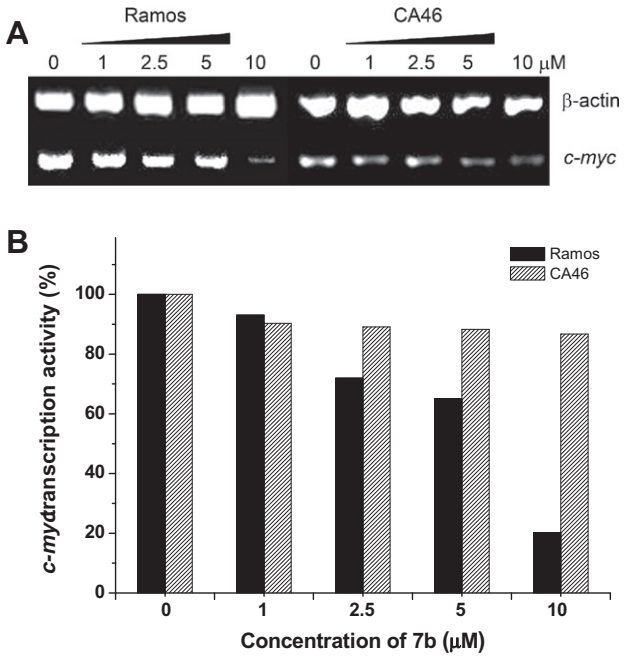

Figure 6. (A) A RT-PCR assay revealed dose-dependent inhibition of *c-myc* transcription by compound **7b** in Ramos and CA46 cells. Amplified products were 191 bp for *c-myc* and 541 bp for β-actin. (B) Relative *c-myc* expression level was measured by using a densitometer.

lines with different translocation break points within the *c-myc* were tested. The Ramos cell line retains the NHE III_1 during translocation, while the CA46 cell line has lost this element together with the P1 and P2 promoters.[40,41] For the CA46 cell line with the NHE III_1 element deleted, **7b** showed no effect on *c-myc* expression, while for the Ramos cell line with this element, **7b** could lower the *c-myc* expression. As shown in Figure 6 and 2.5 μM of **7b** started to inhibit the expression of *c-myc* in Ramos cell line, and could significantly suppress the *c-myc* mRNA level at a concentration of 10 μM.

3. Conclusion

A series of the DPC derivatives were designed, synthesized and found to be selective G-quadruplex binding ligands. The terminal pyrrolidino group was proved to be optimal for G-quadruplex binding, while the terminal morpholine group was proved to be poor for G-quadruplex binding. Further cellular studies showed that all compounds had strong cytotoxicity against cancer cells with low toxicity towards the normal cells. Compound **7b** showed significant inhibition of *c-myc* gene expression in cultured cells, presumably through the stabilization of the *c-myc* G-quadruplex structure. Because of the complicated network of various genes in vivo, the cytotoxicity of the carbazole derivatives against cancer cells may not be limited to their effect on *c-myc* G-quadruplex. Other possible G-quadruplex genomic targets could be involved in drug action. Our previous research reported that the quindoline derivative SYUIQ-05 had relatively stronger binding affinity to *c-myc* G-quadruplex DNA in vitro, and it exhibited its antitumor activity on tumor cells mainly through its interaction with *c-myc* in vivo.[42] The DPC derivatives were identified as G-quadruplex ligand for both telomere and *c-myc*, but these compounds showed much stronger stabilization activities and binding affinities for *c-myc* G-quadruplex rather than telomeric G-quadruplex. To further clarify molecular mechanism for antiproliferative properties of the DPC derivatives, more detailed in vivo investigations are now underway.

4. Experimental section

4.1. Synthesis and characterization

^1H and ^{13}C NMR spectra were recorded using TMS as the internal standard in DMSO-d_6 or $CDCl_3$ with a Bruker BioSpin GmbH spectrometer at 400 MHz and 100 MHz, respectively. Mass spectra (MS) were recorded on a Shimadzu LCMS-2010A instrument with an ESI or ACPI mass selective detector, and high resolution mass spectra (HRMS) were recorded on a Shimadzu LCMS-IT-TOF. Melting points (mp) were determined using a SRS-OptiMelt automated melting point instrument without correction.

4.1.1. 3,6-Dinitro-9*H*-carbazole (2)

A homogeneous mixture of $Cu(NO_3)_2{\cdot}2.5H_2O$ (30 mmol), acetic acid (20 mL), and acetic anhydride (30 mL) was prepared at room temperature. To this solution were added carbazole (25 mmol) in small portions over 10 min. Temperature was maintained at 15–20 °C during addition of carbazole. The temperature was allowed to rise to room temperature over a period of 30 min and then to 90 °C. Reaction was continued with stirring for a period of 30 min at this temperature. The mixture was poured into 250 mL of distilled water with constant stirring. The precipitate was collected by filtration, and washed five times each with about 100 mL of distilled water. The filtrate was dried in vacuumat. Chromatography on silica gel, eluting with petroleum/EtOAC (3:1) gave **2** (5.23 g, 81%) as a yellow solid. mp >300 °C (lit.[27] mp >300 °C). ^1H NMR (400 MHz, DMSO-d_6) δ 12.69 (s, 1H), 9.50 (d, J = 2.1 Hz, 2H), 8.40 (dd, J = 9.0, 2.1 Hz, 2H), 7.77 (d, J = 9.0 Hz, 2H). ESI-MS m/z: 258$[M+H]^+$.

4.1.2. 1,8-Dibromo-3,6-dinitro-9*H*-carbazole (3)

A mixture of 3,6-dinitrocarbazole (9 mmol), bromine (3 mL), and H_2SO_4 (30 mL) was warmed for 15 min at 90 °C. Then additional H_2SO_4 (6 mL) were added. The resulting mixture was heated at 90 °C for 6 h. After cooling to room temperature, the brown reaction mixture was poured onto ice and filtered to provide **3** (2.1 g, 56%) as a yellow-green solid. Mp >300 °C. (lit.[27] mp >300 °C). ^1H NMR (400 MHz, DMSO-d_6) δ 12.72 (s, 1H), 9.49 (d, J = 2.1 Hz, 2H), 8.54 (d, J = 2.1 Hz, 2H). ESI-MS m/z: 416 $[M+H]^+$.

4.1.3. 3,6-Dinitro-1,8-di(1*H*-pyrazol-1-yl)-9*H*-carbazole (4)

A mixture of compound **3** (4.8 mmol), Cu_2O (0.48 mmol) and pyrazole (48 mmol) were heated together with NMP (15 ml) at 200 °C under argon for 24 h. After cooling to room temperature, the mixture was poured into H_2O and filtered to provide a yellow solid. Chromatography on Al_2O_3 basic, eluting with CH_2Cl_2 gave **4** as a yellow-green solid (0.81 g, 43%). Mp >300 °C. ^1H NMR (400 MHz, DMSO-d_6) δ 12.83 (s, 1H), 9.35 (d, J = 1.8 Hz, 2H), 9.02 (d, J = 2.6 Hz, 2H), 8.76 (d, J = 1.9 Hz, 2H), 8.01 (d, J = 1.7 Hz, 2H), 6.74–6.71 (m, 2H). ESI-MS m/z: 390 $[M+H]^+$.

4.1.4. General procedure: preparation of 5a and 5b

Compound **4** (2.0 mmol) were placed into a round-bottom flask together with Sn (metal, 10 mmol), acetic acid (10 mL), and concentrated hydrochloric acid (2.5 mL). The mixture was refluxed for 30 h under a blanket of nitrogen. The resulting solution was cooled, and poured into an aqueous solution of 1.2 g of NaOH in 50 mL of water. The precipitate was filtered, washed free of alkali with water, and dried in vacuum for 24 h. The product was purified by extraction with THF, evaporation of THF under vacuum to give a solid residue (0.48 g, 73%). Then solid residue in chloroacetyl chloride (10 mL) or 3-chloropropionyl chloride (10 mL) was heated at 70 °C for 8 h. After cooling to 0 °C, the mixture was diluted with distilled ether. The resulting solution was filtered, washed with ether and water, and then evaporated under vacuum. The crude solide was chromatographed on silica gel eluting with petroleum/EtOAC (2:1) to give **5a** and **5b**.

4.1.4.1. *N,N'*-(1,8-Di(1*H*-pyrazol-1-yl)-9*H*-carbazole-3,6-diyl)-bis(2-chloroacetamide) (5a). Following General procedure, a white solid **5a** (0.48 g, 68%) was obtained. Mp: 286–287 °C. ^{1}H NMR (400 MHz, DMSO-d_6) δ 11.64 (s, 1H), 10.54 (s, 2H), 8.59 (d, J = 2.5 Hz, 2H), 8.35 (d, J = 1.3 Hz, 2H), 8.02 (d, J = 1.7 Hz, 2H), 6.73–6.71 (m, 2H), 4.36 (s, 4H). ESI-MS m/z: 482 $[M+H]^+$.

4.1.4.2. *N,N'*-(1,8-Di(1*H*-pyrazol-1-yl)-9*H*-carbazole-3,6-diyl)bis (3-chloropropanamide) (5b). Following General procedure, a white solid **5b** (0.45 g, 61%) was obtained. mp: 268–269 °C. ^{1}H NMR (400 MHz, DMSO-d_6) δ 11.55 (s, 1H), 10.29 (s, 2H), 8.53 (d, J = 2.4 Hz, 2H), 8.34 (d, J = 1.5 Hz, 2H), 8.01 (d, J = 1.8 Hz, 2H), 8.01 (d, J = 1.6 Hz, 2H), 6.72–6.68 (m, 2H), 3.96 (t, J = 6.3 Hz, 4H), 2.91 (t, J = 6.3 Hz, 4H). ESI-MS m/z: 510 $[M+H]^+$.

4.1.5. General procedure: preparation of 6a–d, and 7a–d

To a stirred suspension of the chloride compounds **5a** or **5b** (0.3 mmol) in EtOH (25 mL) was added dropwise appropriate amine (2.0 mL) in EtOH (5 mL). The mixture was stirred and heated under reflux for 8–12 h, and the reaction was monitored periodically by using TLC, cooled to 0 °C, and diluted with distilled water. The resulting solution was filtered, washed with ether and water, then evaporated under vacuum. The crude solid was purified by using Al_2O_3 with $CHCl_2$/MeOH (50:1–20:1) elution to afford **6a–d** and **7a–d**.

4.1.5.1. *N,N'*-(1,8-Di(1*H*-pyrazol-1-yl)-9H-carbazole-3,6-diyl)-bis(2-(pyrrolidin-1-yl)acetamide) (6a). Compound **5a** was treated with pyrrolidine following the general procedure to give the desired product **6a** as a white solid with a yield of 22%. Mp 245–247 °C. ^{1}H NMR (400 MHz, DMSO-d_6) δ 11.58 (s, 1H), 9.80 (s, 2H), 8.59 (d, J = 2.4 Hz, 2H), 8.49 (d, J = 1.2 Hz, 2H), 8.08 (d, J = 1.5 Hz, 2H), 8.00 (d, J = 1.5 Hz, 2H), 6.71–6.68 (m, 2H), 3.33 (s, 4H), 2.69–2.66 (m, 8H), 1.83–1.79 (m, 8H). ^{13}C NMR (101 MHz, DMSO-$d6$) δ 168.98, 141.15, 131.38, 128.23, 126.87, 124.45, 123.87, 109.35, 108.51, 107.66, 59.64, 53.85, 23.56. ESI-HRMS m/z: calcd for $C_{30}H_{33}N_9O_2$ $[M+H]^+$ 552.2830, found 552.2848.

4.1.5.2. *N,N'*-(1,8-Di(1*H*-pyrazol-1-yl)-9*H*-carbazole-3,6-diyl)-bis(2-(piperidin-1-yl)acetamide) (6b). Compound **5a** was treated with piperidine following the general procedure to give the desired product **6b** as a white solid with a yield of 55%. Mp 160–162 °C. ^{1}H NMR (400 MHz, DMSO-d_6) δ 11.59 (s, 1H), 9.76 (s, 2H), 8.61 (d, J = 2.4 Hz, 2H), 8.48 (d, J = 1.3 Hz, 2H), 8.06 (d, J = 1.5 Hz, 2H), 8.00 (d, J = 1.6 Hz, 2H), 6.71–6.67 (m, 2H), 3.14 (s, 4H), 2.56–2.52 (m, 8H), 1.67–1.61 (m, 8H), 1.47–1.41 (m, 4H). ^{13}C NMR (101 MHz, $CDCl_3$) δ 167.86, 140.02, 129.2, 127.96, 126.38, 124.25, 123.74, 108.26, 107.03, 106.15, 61.84, 54.04, 25.34, 22.65. ESI-HRMS m/z: calcd for $C_{32}H_{37}N_9O_2$ $[M+H]^+$ 580.3143, found 580.3169.

4.1.5.3. *N,N'*-(1,8-Di(1*H*-pyrazol-1-yl)-9*H*-carbazole-3,6-diyl)-bis(2-(diethylamino)acetamide) (6c). Compound **5a** was treated with diethylamine following the general procedure to give the desired product **6c** as a white solid with a yield of 23%. Mp 151–153 °C. ^{1}H NMR (400 MHz, DMSO-d_6) δ 11.61 (s, 1H), 9.80 (s, 2H), 8.63 (d, J = 2.5 Hz, 2H), 8.54 (d, J = 1.3 Hz, 2H), 8.10 (d, J = 1.6 Hz, 2H), 8.00 (d, J = 1.7 Hz, 2H), 6.72–6.68 (m, 2H), 3.23 (s, 4H), 2.68 (q, J = 7.1 Hz, 8H), 1.09 (q, J = 7.1 Hz, 12H). ^{13}C NMR (101 MHz, $CDCl_3$) δ 169.11, 140.00, 129.24, 127.90, 126.37, 124.22, 123.72, 108.10, 106.92, 106.13, 57.14, 47.98, 11.51. ESI-HRMS m/z: calcd for $C_{30}H_{37}N_9O_2$ $[M+H]^+$ 556.3143, found 556.3168.

4.1.5.4. *N,N'*-(1,8-Di(1*H*-pyrazol-1-yl)-9*H*-carbazole-3,6-diyl)-bis(2-morpholinoacetamide) (6d). Compound **5a** was treated with morpholine following the general procedure to give the desired product **6d** as a white solid with a yield of 39%. Mp 250–251 °C. ^{1}H NMR (400 MHz, DMSO-d_6) δ 11.60 (s, 1H), 9.85 (s, 2H), 8.60 (d, J = 2.4 Hz, 2H), 8.45 (d, J = 1.3 Hz, 2H), 8.05 (d, J = 1.5 Hz, 2H), 8.00 (d, J = 1.5 Hz, 2H)), 6.73–6.70 (m, 2H), 3.71 (t, J = 4.0 Hz, 8H), 3.21 (s, 4H), 2.58 (t, J = 4.0 Hz,8H); ^{13}C NMR (101 MHz, $CDCl_3$) δ 166.89, 140.12, 128.97, 128.05, 126.36, 124.20 123.80, 108.36, 107.09, 106.27, 66.08, 61.54, 52.92. ESI-HRMS m/z: calcd for $C_{30}H_{33}N_9O_4$ $[M+H]^+$ 584.2728, found 584.2738.

4.1.5.5. *N,N'*-(1,8-Di(1*H*-pyrazol-1-yl)-9*H*-carbazole-3,6-diyl)-bis(3-(pyrrolidin-1-yl)propanamide) (7a). Compound **5b** was treated with pyrrolidine following the general procedure to give the desired product **7a** as a white solid with a yield of 32%. Mp 263–265 °C; ^{1}H NMR (400 MHz, DMSO-d_6) δ 11.49 (s, 1H), 10.23 (s, 1H), 8.51 (d, J = 2.1 Hz, 2H), 8.31 (d, J = 1.3 Hz, 2H), 7.99 (d, J = 1.6 Hz, 2H), 7.98 (d, J = 1.5 Hz, 2H), 6.71–6.67 (m, 2H), 2.79 (t, J = 7.0 Hz, 4H), 2.56 (t, J = 7.0 Hz, 4H), 2.54–2.51 (m, 8H), 1.73–1.70 (m, 8H); ^{13}C NMR (101 MHz, $CDCl_3$) δ 169.88, 139.95, 130.08, 127.79, 126.31, 124.16, 123.60, 108.53, 107.63, 106.07, 52.28, 50.58, 33.65, 22.81. ESI-HRMS m/z: calcd for $C_{32}H_{37}N_9O_2$ $[M+H]^+$ 580.3143, found 580.3144.

4.1.5.6. *N,N'*-(1,8-Di(1*H*-pyrazol-1-yl)-9*H*-carbazole-3,6-diyl)-bis(3-(piperidin-1-yl)propanamide) (7b). Compound **5b** was treated with piperidine following the general procedure to give the desired product **7b** as a white solid with a yield of 42%. Mp 166–167 °C.^{1}H NMR (400 MHz, DMSO-d_6) δ 11.49 (s, 1H), 10.29 (s, 2H), 8.50 (d, J = 2.5 Hz, 2H), 8.28 (d, J = 1.5 Hz, 2H), 7.99 (d, J = 1.7 Hz, 2H), 7.97 (d, J = 1.6 Hz, 2H), 6.71–6.68 (m, 2H), 2.67 (t, J = 6.9 Hz, 4H), 2.53 (t, J = 6.9 Hz, 4H), 2.45–2.41 (m, 8H), 1.55–1.52 (m, 8H), 1.44–1.40 (m, 4H). ^{13}C NMR (101 MHz, $CDCl_3$) δ 169.79, 139.92, 130.24, 127.71, 126.29, 124.11, 123.59, 107.95, 107.40, 106.07, 53.45, 52.70, 31.53, 25.31, 23.24. ESI-HRMS m/z: calcd for $C_{34}H_{41}N_9O_2$ $[M+H]^+$ 608.3456, found 608.3479.

4.1.5.7. *N,N'*-(1,8-Di(1*H*-pyrazol-1-yl)-9*H*-carbazole-3,6-diyl)-bis(3-(diethylamino)propanamide) (7c). Compound **5b** was treated with diethylamine following the general procedure to give the desired product **7c** as a white solid with a yield of 53%. Mp 271–272 °C. ^{1}H NMR (400 MHz, $CDCl_3$) δ 11.44 (s, 1H), 11.24 (s, 2H), 8.04 (d, J = 2.0 Hz, 2H), 7.92–7.89 (m, 4H), 7.82 (d, J = 1.7 Hz, 2H), 6.48–6.44 (m, 2H), 2.81 (t, J = 5.8 Hz, 4H), 2.70 (q, J = 7.1 Hz, 8H), 2.54 (t, J = 5.8 Hz, 4H), 1.13 (t, J = 7.1 Hz, 12H). ^{13}C NMR (101 MHz, CDCl3) δ 169.36, 139.86, 129.84, 127.63, 126.29, 124.10, 123.41, 108.64, 107.57, 106.02, 47.82, 45.19, 31.90, 28.67 9.77. ESI-HRMS m/z: calcd for $C_{32}H_{41}N_9O_2$ $[M+H]^+$ 584.3456, found 584.3468.

4.1.5.8. *N,N'*-(1,8-Di(1*H*-pyrazol-1-yl)-9*H*-carbazole-3,6-diyl)-bis(3-morpholinopropanamide) (7d). Compound **5b** was treated with morpholine following the general procedure to give the desired product **7d** as a white solid with a yield of 25%. Mp 264–266 °C; ^{1}H NMR (400 MHz, DMSO-d_6): δ 11.51 (s, 1H), 10.23 (s, 2H), 8.52 (d, J = 2.2 Hz, 2H), 8.32 (d, J = 1.5 Hz, 2H), 8.00 (d, J = 1.5 Hz, 2H), 7.97 (d, J = 1.5 Hz, 2H), 6.69–6.72 (m, 2H), 3.59 (t, J = 4.2 Hz, 8H), 2.70 (t, J = 6.8 Hz, 4H), 2.56 (t, J = 6.8 Hz, 4H), 2.45 (t, J = 4.2 Hz, 8H). ^{13}C NMR (101 MHz, $CDCl_3$) δ 169.31, 140.04, 129.78, 127.97, 126.28, 124.44, 123.45, 108.36, 107.55, 106.21, 66.07, 53.31, 51.92, 31.31. ESI-HRMS m/z: calcd for $C_{32}H_{37}N_9O_4$ $[M+H]^+$ 612.3041, found 612.3052.

4.2. Biological assays

4.2.1. FRET-melting assay

FRET assay was carried out on a real-time PCR apparatus following previously published procedures. The fluorescently labeled oligonucleotides FPu18T (5′-FAM-AGGGTGGGGA-GGGTGGGG-TAMRA-3′), F21T (5′-FAM-d(GGG[TTAGGG]$_3$)-TAMRA-3′) and F10T: 5′-FAM-dTAT-AGCTATA-HEG-TATAGCTATA-TAMRA-3′ (donor fluorophore FAM is 6-carboxy-fluorescein; acceptor fluorophore TAMRA is 6-carboxytetramethyl-rhodamine; HEG linker is [(–CH_2–CH_2–O–)$_6$]) were used as the FRET probes. Fluorescence melting curves were determined with a Roche LightCycler 2 real-time PCR machine, using a total reaction volume of 20 μL, with 0.2 μM of labeled oligonucleotide in Tris–HCl buffer (10 mM, pH 7.2) containing 0.2 mM or 60 mM KCl. Fluorescence readings with excitation at 470 nm and detection at 530 nm were taken at intervals of 1 °C over the range 37–99 °C, with a constant temperature being maintained for 30 s prior to each reading to ensure a stable value. The melting of the G-quadruplex was monitored alone or in the presence of various concentrations of compounds and/or of double-stranded competitor ds26 (ds26 DNA: 5′-GTTAGCCTAGCTT AAGCTAGGCTAAC-3′). Final analysis of the data was carried out using Origin8.0 (OriginLab Corp.).

4.2.2. Surface Plasmon Resonance

SPR measurements were performed on a ProteOn XPR36 Protein Interaction Array system (Bio-Rad Laboratories, Hercules, CA) using a Neutravidin-coated GLH sensor chip. In a typical experiment, biotinylated duplex DNA, biotinylated HTG21 and biotinylated Pu18 were folded in filtered and degassed running buffer (Tris–HCl, 50 mM, pH 7.2, 100 mM KCl). The DNA samples were then captured (−1000 RU) in flow cells 1 and 2, leaving the third flow cell as a blank. Ligand solutions (at 0.3125, 0.625, 1.25, 2.5, 5, 10 μM) were prepared with running buffer by serial dilutions from stock solutions. Six concentrations were injected simultaneously at a flow rate of 100 mL min^{-1} for 150 s of association phase, followed with 300 s of dissociation phase at 25 °C. The GLH sensor chip was regenerated with short injection of 1 M NaCl between consecutive measurements. The final graphs were obtained by subtracting blank sensorgrams from the duplex or quadruplex sensorgrams. Data were analyzed with ProteOn manager software, using the Langmuir model for fitting kinetic data.

4.2.3. CD measurements

The oligomer Pu18 (5′-AGGGTGGGGAGGGTGGGG-3′) at a final concentration of 5 μM was resuspended in Tris–HCl buffer (10 mM, pH 7.2) containing the derivatives to be tested. The samples were heated to 95 °C, then gradually cooled to room temperature, and incubated at 4 °C for at least 6 h. The CD spectra were recorded on a Chirascan (AppliedPhotophysics) spectrophotometer, using 0.5 s-per-points from 220 to 450 nm and 1 nm bandwidth. The CD spectra were obtained by averaging two scans. Final analysis of the data was carried out using Origin 8.0 (Originlab Corp.).

4.2.4. Molecular modeling

The previously built Pu-18B G-quadruplex structure was used as the initial model to study the interactions between compounds and human *c-myc* G-quadruplex.[37] Ligand structures were constructed by adopting the empirical Gasteiger–Huckel (GH) partial atomic charges, and then were optimized (Tripos force field) with a nonbond cutoff of 12 Å and a convergence of 0.01 kcal mol^{-1}/Å over 10,000 steps using the Powell conjugate-gradient algorithm. Docking studies were carried out using the AUTODOCK 4.0 program. The G-quadruplex structure was used as an input for the AUTOGRID program. The grid box was placed at the center of the G-quadruplex. The dimensions of the active site box were set at 60 × 60 × 60 Å. Docking calculations were carried out using the Lamarckian genetic algorithm (LGA). Initially, we used a population of random individuals (population size: 150), a maximum number of 25,000,000 energy evaluations, a maximum number of generations of 27,000, and a mutation rate of 0.02. Hundred independent docking runs were carried out for each ligand. The resulting positions were clustered according to a root-mean-square criterion of 0.5 Å.

4.2.5. PCR-stop assay

The polymerase stop assay was performed as described previously.[37] Sequences of the tested oligomers were Pu27 (5′-TG GGGAGGGTGGGGAGGGTGGGG-AAGG-3′) and the corresponding complementary sequence. The reactions were performed in 1 × PCR buffer, containing 10 μM of each pair of oligomers, 0.16 mM dNTP, 2.5 U *Taq* polymerase, and the indicated amount of the compounds. Reaction mixtures were incubated in a thermocycler, with the following cycling conditions: 94 °C for 3 min, followed with 30 cycles of 94 °C for 30 s, 5 °C for 30 s, and 72 °C for 30 s. Amplified products were resolved on 15% nondenaturing polyacrylamide gels in 1 × TBE and silver stained.

4.2.6. Cell culture

HL60 leukemia cell line, ECV-304 epithelial cell, HepG2 hepatoma cell line, NCI-H460 lung cancer, Ramos, and CA46, were obtained from the Experimental Animal Center of Sun Yat-sen University. The cell cultures were maintained in RPMI-1640 medium supplemented with fetal bovine serum (10%), glutamine (1%), Penicillin (100 U/mL) and Streptomycin (1%) in 25 cm^2 culture flasks at 37 °C in a humidified atmosphere with 5% CO_2.

4.2.7. MTT assay

HL60 leukemia cell line, ECV-304 epithelial cell, HepG2 hepatoma cell line and NCI-H460 lung cancer cell line were seeded on 96-well plates (1.0 × 10^3/well), and exposed to various concentrations of derivatives. After 48 h of treatment at 37 °C in a humidified atmosphere of 5% CO_2, 10 μL of 5 mg/mL methyl thiazolyl tetrazolium (MTT) solution was added to each well and further incubated for 4 h. The cells in each well were then treated with dimethyl sulfoxide (DMSO) (200 μL for each well), and the optical density (OD) was recorded at 570 nm. All drug doses were parallel tested in triplicate, and the IC_{50} values were derived from the mean OD values of the triplicate tests versus drug concentration curves.

4.2.8. RNA extraction

Ramos and CA46 cells were seeded in six-well plates at 100,000 cells/well, and compounds were added at final concentration of 1, 2.5, 5, 10 μM or DMSO control. After incubation for 4 days, cells were harvested, and the RNA was extracted according to the manufacturer's instructions. Cell pellets harvested from each well of the culture plates were lysed in Redzol solution. RNA was extracted with M-MLV according to manufacturer's protocol, and eluted in distilled, deionized water with 0.1% diethyl pyrocarbonate (DEPC) to a final volume of 10–50 mL. RNA was quantitated spectrophotometrically and stored at −80 °C.

4.2.9. RT-PCR

The quantity of the RNA was measured by using UV spectrometry. Synthesis of cDNA was performed using 2 μg of total RNA. Total RNA was used as a template for reverse transcription using the following protocol: each 20 μL reaction contained 5 × M-MLV buffer, 2.5 mM dNTP, 50 μM oligo dT_{18} primer, 1 μL M-MLV reverse transcriptase, DEPC in water (DEPC H_2O), and 2 μg of total RNA. Briefly, RNA and oligo dT_{18} primer was incubated at 70 °C for 10 min and then immediately placed on ice, after which the other components were added and incubated at 42 °C for 1 h and then at 70 °C for 15 min. Finally, the reacted solution was stored at −20 °C. For each cDNA sample, one 20 μL reaction was set up on ice, containing 10 × PCR buffer, 2.5 mM dNTP, primer c-mycA, primer c-mycS, and rTaq. Both *c-myc* and β-actin were amplified by using PCR, and the PCR products were analyzed by using electrophoresis on 1% agarose gel at 120 V for 20 min. Photograghs were taken with multilmage light cabinet. The quantity of the *c-myc* expression was normalized based on the control gene β-actin, and the expression of *c-myc* in Ramos cells was compared with the expression of *c-myc* in CA46 cells.

Conflict of interest

We declare that we have no conflict of interest.

Acknowledgements

This work was supported by National Natural Science Foundation of China (Nos. U0832005, 90813011, 21172272, 81001400), the International S&T Cooperation Program of China (No. 2010DFA34630).

Supplementary data

Supplementary data associated with this article can be found, in the online version, at http://dx.doi.org/10.1016/j.bmc.2012.03.031.

References and notes

1. Simonsson, T. *Biol. Chem.* **2001**, *382*, 621.
2. Huppert, J. L.; Balasubramanian, S. *Nucleic Acids Res.* **2007**, *35*, 406.
3. Blackburn, E. H. *Nature* **1991**, *350*, 569.
4. De Cian, A.; Lacroix, L.; Douarre, C.; Temime-Smaali, N.; Trentesaux, C.; Riou, J. F.; Mergny, J. L. *Biochimie* **2008**, *90*, 131.
5. Neidle, S.; Parkinson, G. *Nat. Rev. Drug Disc.* **2002**, *1*, 383.
6. Arora, A.; Dutkiewicz, M.; Scaria, V.; Hariharan, M.; Maiti, S.; Kurreck, J. *RNA* **2008**, *14*, 1290.
7. Balasubramanian, S.; Hurley, L. H.; Neidle, S. *Nat. Rev. Drug Disc.* **2011**, *10*, 261.
8. Postel, E. H.; Mango, S. E.; Flint, S. J. *Mol. Cell. Biol.* **1989**, *9*, 5123.
9. Davis, T. L.; Firulli, A. B.; Kinniburgh, A. J. *Proc. Natl. Acad. Sci. U.S.A.* **1989**, *86*, 9682.
10. Seenisamy, J.; Bashyam, S.; Gokhale, V.; Vankayalapati, H.; Sun, D.; Siddiqui-Jain, A.; Streiner, N.; Shin-Ya, K.; White, E.; Wilson, W. D.; Hurley, L. H. *J. Am. Chem. Soc.* **2005**, *127*, 2944.
11. Lu, Y. J.; Ou, T. M.; Tan, J. H.; Hou, J. Q.; Shao, W. Y.; Peng, D.; Sun, N.; Wang, X. D.; Wu, W. B.; Bu, X. Z.; Huang, Z. S.; Ma, D. L.; Wong, K. Y.; Gu, L. Q. *J. Med. Chem.* **2008**, *51*, 6381.
12. Wu, P.; Ma, D. L.; Leung, C. H.; Yan, S. C.; Zhu, N.; Abagyan, R.; Che, C. M. *Chemistry* **2009**, *15*, 13008.
13. Patel, D. J.; Phan, A. T.; Kuryavyi, V. *Nucleic Acids Res.* **2007**, *35*, 7429.
14. Monchaud, D.; Teulade-Fichou, M. P. *Org. Biomol. Chem.* **2008**, *6*, 627.
15. Moorhouse, A. D.; Haider, S.; Gunaratnam, M.; Munnur, D.; Neidle, S.; Moses, J. E. *Mol. Biosyst.* **2008**, *4*, 629.
16. Taufiq-Yap, Y. H.; Peh, T. H.; Ee, G. C.; Rahmani, M.; Sukari, M. A.; Ali, A. M.; Muse, R. *Nat. Prod. Res.* **2007**, *21*, 810.
17. Songsiang, U.; Thongthoom, T.; Boonyarat, C.; Yenjai, C. *J. Nat. Prod.* **2011**, *74*, 208.
18. Huang, F. C.; Chang, C. C.; Lou, P. J.; Kuo, I. C.; Chien, C. W.; Chen, C. T.; Shieh, F. Y.; Chang, T. C.; Lin, J. J. *Mol. Cancer Res.* **2008**, *6*, 955.
19. Ou, T. M.; Lu, Y. J.; Tan, J. H.; Huang, Z. S.; Wong, K. Y.; Gu, L. Q. *ChemMedChem* **2008**, *3*, 690.
20. Tan, J. H.; Gu, L. Q.; Wu, J. Y. *Mini-Rev. Med. Chem.* **2008**, *8*, 1163.
21. Labbozzetta, M.; Baruchello, R.; Marchetti, P.; Gueli, M. C.; Poma, P.; Notarbartolo, M.; Simoni, D.; D'Alessandro, N. *Chem. Biol. Interact.* **2009**, *181*, 29.
22. Pevarello, P.; Brasca, M. G.; Amici, R.; Orsini, P.; Traquandi, G.; Corti, L.; Piutti, C.; Sansonna, P.; Villa, M.; Pierce, B. S.; Pulici, M.; Giordano, P.; Martina, K.; Fritzen, E. L.; Nugent, R. A.; Casale, E.; Cameron, A.; Ciomei, M.; Roletto, F.; Isacchi, A.; Fogliatto, G.; Pesenti, E.; Pastori, W.; Marsiglio, A.; Leach, K. L.; Clare, P. M.; Fiorentini, F.; Varasi, M.; Vulpetti, A.; Warpehoski, M. A. *J. Med. Chem.* **2004**, *47*, 3367.
23. Tanitame, A.; Oyamada, Y.; Ofuji, K.; Terauchi, H.; Kawasaki, M.; Wachi, M.; Yamagishi, J. *Bioorg. Med. Chem. Lett.* **2005**, *15*, 4299.
24. Szabo, G.; Fischer, J.; Kis-Varga, A.; Gyires, K. *J. Med. Chem.* **2008**, *51*, 142.
25. Tanitame, A.; Oyamada, Y.; Ofuji, K.; Fujimoto, M.; Suzuki, K.; Ueda, T.; Terauchi, H.; Kawasaki, M.; Nagai, K.; Wachi, M.; Yamagishi, J. *Bioorg. Med. Chem.* **2004**, *12*, 5515.
26. Maity, S. C.; Mal, D.; Maiti, M. M. *Thermochim. Acta* **2005**, *435*, 135.
27. Gu, R.; Hameurlaine, A.; Dehaen, W. *J. Org. Chem.* **2007**, *72*, 7207.
28. Roland, J. P.; Julius, R. *J. Recuril. Des. Travaux. Chimiques. Des. Pays-Bas.* **1993**, *112*, 330.
29. Rachwal, P. A.; Fox, K. R. *Methods* **2007**, *43*, 291.
30. Bejugam, M.; Sewitz, S.; Shirude, P. S.; Rodriguez, R.; Shahid, R.; Balasubramanian, S. *J. Am. Chem. Soc.* **2007**, *129*, 12926.
31. Waller, Z. A. E.; Shirude, P. S.; Rodriguez, R.; Balasubramanian, S. *Chem. Commun.* **2008**, 1467.
32. Rossetti, L.; Franceschin, M.; Schirripa, S.; Bianco, A.; Ortaggi, G.; Savino, M. *Bioorg. Med. Chem. Lett.* **2005**, *15*, 413.
33. Moorhouse, A. D.; Santos, A. M.; Gunaratnam, M.; Moore, M.; Neidle, S.; Moses, J. E. *J. Am. Chem. Soc.* **2006**, *128*, 15972.
34. De Cian, A.; DeLemos, E.; Mergny, J. L.; Teulade-Fichou, M. P.; Monchaud, D. *J. Am. Chem. Soc.* **2007**, *129*, 1856.
35. Redman, J. E. *Methods* **2007**, *43*, 302.
36. Paramasivan, S.; Rujan, I.; Bolton, P. H. *Methods* **2007**, *43*, 324.
37. Ou, T. M.; Lu, Y. J.; Zhang, C.; Huang, Z. S.; Wang, X. D.; Tan, J. H.; Chen, Y.; Ma, D. L.; Wong, K. Y.; Tang, J. C.; Chan, A. S.; Gu, L. Q. *J. Med. Chem.* **2007**, *50*, 1465.
38. DeLano, W. L. *The PyMOL Molecular Graphics System*; DeLano Scientific: San Carlos, CA, 2002.
39. Lemarteleur, T.; Gomez, D.; Paterski, R.; Mandine, E.; Mailliet, P.; Riou, J. F. *Biochem. Biophys. Res. Commun.* **2004**, *323*, 802.
40. Facchini, L. M.; Penn, L. Z. *FASEB J.* **1998**, *12*, 633.
41. Simonsson, T.; Henriksson, M. *Biochem. Biophys. Res. Commun.* **2002**, *290*, 11.
42. Ou, T.-M.; Lin, J.; Lu, Y.-J.; Hou, J.-Q.; Tan, J.-H.; Chen, S.-H.; Li, Z.; Li, Y.-P.; Li, D.; Gu, L.-Q.; Huang, Z.-S. *J. Med. Chem.* **2011**, *54*, 5671.